World Journal of Environmental Engineering, 2017, Vol. 5, No. 1, 7-16
Available online at http://pubs.sciepub.com/wjee/5/1/2

DOI:10.12691/wjee-5-1-2

Rock Fracture Characterization for Solid Waste Disposal Site Selection: A Case from Sites in the Accra-Tema Area, SE Ghana

Amadu Casmed Charles[1,*], Foli Gordon[2], Abanyie Samuel[1]

[1]Earth and Environmental Sciences Department, University for Development Studies (UDS), Navrongo, Ghana
[2]Department of Geological Engineering, Kwame Nkrumah University of Science and Technology (KNUST), Kumasi, Ghana
*Corresponding author: camadudu@uds.edu.gh

Abstract In this paper, information on fracture characteristics in representatively selected sites in the Togo Structural Units (TSU) and Dahomeyan Formation in southeastern Ghana is presented. The study area is locatedat the south most edge of the Pan-African Dahomeyide belt, characterised by intense fracturing. Linear and circular scanline mappings, structural geological mapping, and laboratory investigations of rock samples collected from Site 1 (within the TSU), and Site 2(within the Dahomeyan Formation) were carried out. A total of 1128 fractures were surveyed along a total length of 238 m of scanline at Site 1, and 629 fractures along a total of 156.0 m at Site 2. Fourteen and thirteen circular scanlines were surveyed at Site 1and Site 2 respectively. Statistical analysis of fracture data from the two study sites, and comparing the mean fracture spacing to International Society for Rock Mechanics (ISRM) indicated a close to moderate fracture spacing for the two sites. However, fracturing is more intense in the TSU than the Dahomeyan formation, probably due to the nature of the major rock types, and difference in thickness of the two stratigraphic units. Micro-structural investigation on rock samples also showed mineral grains in the rocks of the TSU are more deformed compared to those of the Dahomeyan. Implications are that, potential for fluid flow and contaminants resulting from waste disposal could travel faster and for wider distances within Site 1 than in Site 2. Site 2 thus, could be a better choice for waste disposal site selection compared to Site 1due to its lesser fractured nature, and the fact that, the Dahomeyan already has natural groundwater quality problems.

Keywords: *waste disposal site selection, environmental hydrogeology, Accra-Tema area (Ghana)*

Cite This Article: Amadu Casmed Charles, Foli Gordon, and Abanyie Samuel, "Rock Fracture Characterization for Solid Waste Disposal Site Selection: A Case from Sites in the Accra-Tema Area, SE Ghana." *World Journal of Environmental Engineering*, vol. 5, no. 1 (2017): 7-16. doi: 10.12691/wjee-5-1-2.

1. Introduction

Waste disposal is an increasing problem throughout the world. Waste is generated universally, and is a direct consequence of all manner of human activities. Waste requiring disposal management may be classified into solid, liquid and gaseous or some combination of any of the above [1,2,3]. Solid wastes are mainly disposed of to landfills, because they appear to be the simplest, cheapest and most cost-effective approach [4].

The fate of the waste in the repository can become an issue, since some transformations within the landfill may cause the waste to leach toxic substance into nearby waterbodies that can pose health problems for user communities. It is therefore imperative, that pragmatic efforts are made to select the most suitable sites for the disposal of the waste. Factors relevant for selection of solid waste disposal site include; cost of operation of the disposal site and environmental concerns such as susceptibility of groundwater contamination [5].

In Ghana, and in particular, within Greater Accra Metropolitan area (GAMA), there are several active and abandoned waste disposal sites. Location of the sites is more often determined by access to collection vehicles and availability of space rather than ecological, environmental or public health and property considerations [6]. This is probably due to lack of policies for realistic long-term planning and monitoring programmes to serve as checks on groundwater pollution from these dump sites, some of which pose a significant environmental threat in polluting groundwater and surface water [7].

The extent and amount of groundwater contamination depends on, the amounts and types of wastes deposited, site management, and site location in relation to aquifer groundwater vulnerability. Within the GAMA, particularly in the peri-urban and rural areas, residents depend on groundwater as the main source of water supply. In many regions of the world, groundwater is limited by quality rather than quantity [8].

Management of groundwater contamination from dump sites can be achieved by the selection of suitable natural sites, based on proven geological and hydrogeological characterisation. Varying criteria for site selection purposes abound because of equally varying regional site conditions [9,10]. According to Paraskevopoulos et al., [11]; Petts and Eduljee, [12] some of the factors which

determine the suitability of waste disposal sites are 1) Characteristics of bedrock lithology, 2) Geological structure, 3) Nature and thickness of unconsolidated material, and 4) Hydro-geological factors.

An optimal waste disposal site is expected to have a low permeable thick cover unit and bedrock that is devoid of discontinuities such as fractures and cleavages, sandwiched by thick unsaturated zone [13]. Fractures result in contaminant transport in unexpected directions, depending on the fracture planes that are intersected. It is a complex factor in relation to predicting the fate and the remediation of groundwater contamination. The focus of this study was to carry out fracture measurement and characterisation in selected sites in the Togo structural unit (TSU) and the Dahomeyan gneissic complex (DGC), of South-eastern Ghana for the purpose of determining the most suitable waste disposal site, using surface linear and circular surveys together with structural mapping.

2. The Study Area

Two study areas located in the Greater Accra Region of Ghana, between latitudes 5º 30¹ 0¹¹ N and 5º 49¹ 0¹¹, and longitudes 0º 8¹ 00¹¹ W and 0º 20¹ 00¹¹ W were selected. Site 1 is located in Ablekuma settlement area within the TSU, and Site 2 is Danfa settlement area, within the DGC. The study locations are presented in Figure 1.

The zone exhibits a double maxima rainfall regime with an annual rainfall between 1145 and 1650 mm. The major and minor rainy seasons are respectively from April to July, and September to November, while the dry season ranges from December to February [14]. The average monthly temperature occur from 28.4°C to 25.1°C in February to August, respectively, while average relative humidity also varies between 65% in the dry season to about 95% in the rainy season [14,15]. The vegetation is of the coastal savannah grassland type [16].

The study area is underlain by metamorphic rocks of the Togo structural unit (TSU) and Dahomeyan gneissic complex (DGC). The main rock units of the TSU are the quartzites, phyllites and schist, where groundwater occurrence depends on secondary porosity resulting from fracturing and weathering [17]. The DGC rocks, consist of acidic and basic gneisses [17], that are generally massive with only few discontinuities, low transmissivity and permeability when compared to the TSU [18].

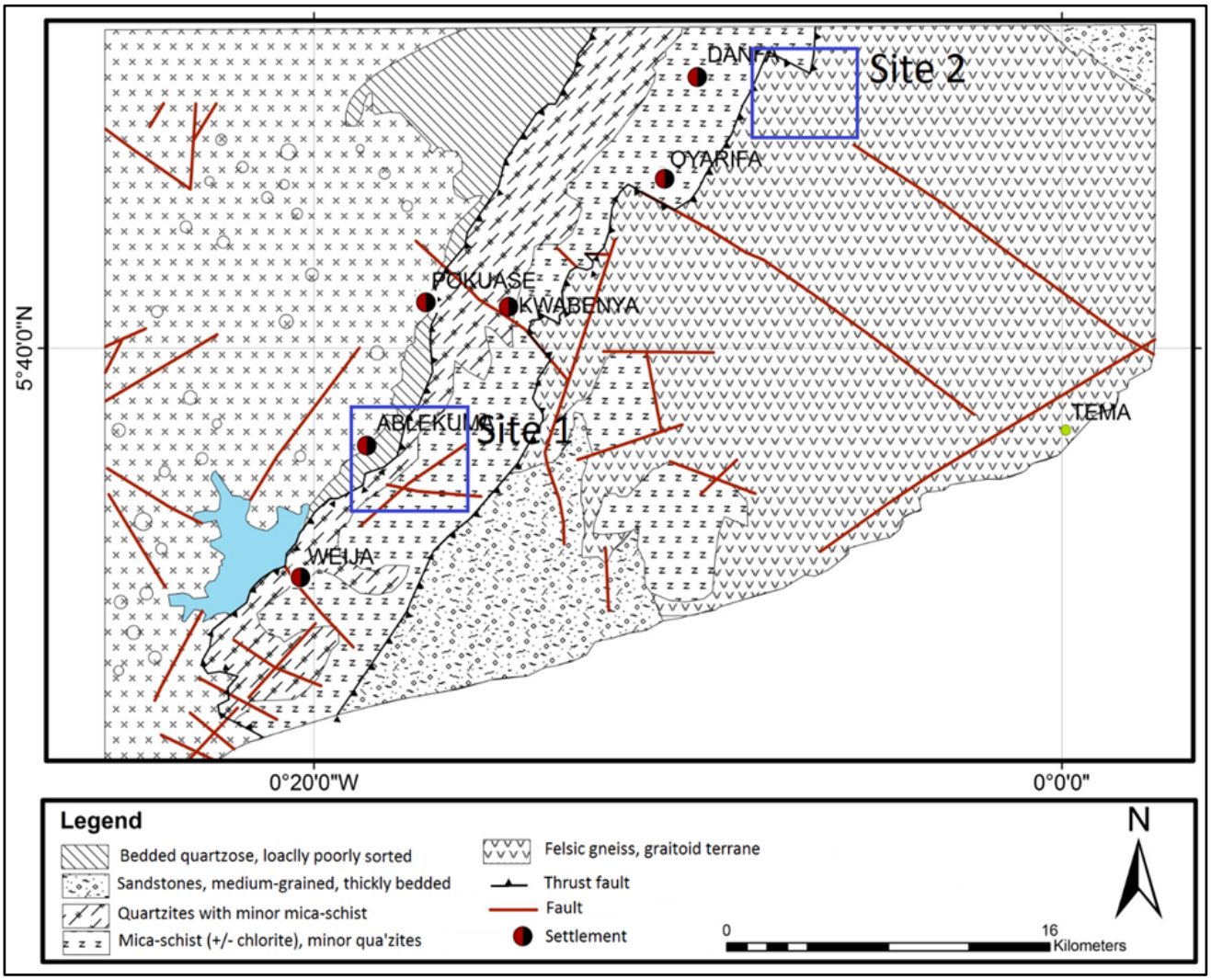

Figure 1. Sketch Map of part of South-eastern Ghana showing location of Study Sites (Modified from [15])

The rock types of the TSU decomposes into clay with varying degree of sand and rock fragments, and has good to moderate groundwater potential [17,18,19]. The average water yielding capacities of boreholes (33-55m) within the TSU is on the average 9.50 m^3/hr [20]. Within the DGC, silicic gneiss weather to form slightly permeable clayey sand, while the basic gneiss also weather to impermeable calcareous clay materials; borehole data indicate yield range between 1.0 to 3.0 m^3/hr, in borehole depths ranging between 45 to 70 m [20].

3. Materials and Methods

3.1. Preliminary Work

Detailed mapping of structures was done, during which hand specimens of the major rock types collected for preparation of thin sections for petro-structural analysis. Traverses were made approximately perpendicular to the general north-eastern strike direction of the rock formations. Structures observed included, foliation, bedding, faults, joints, and quartz veins of varying sizes. For each of the structural features, the location, dip, dip direction and strike were recorded using the Freiberg compass, while location coordinates were recorded using the Garmin Global Positioning system (GPS).

3.2. Fracture Data Collection

Fracture attributes were described and collated in outcrops using 1D (linear) and/or 2D (circular) scanline sampling methods [21,22]. The linear scanline approach consist of measuring fracture spacing and attributes, along a line oriented perpendicular to maximum number of fractures, which are in most cases, parallel to the bedding. Hand specimen description covered rock type, colour, grain size and weathering. In this study, the length of scanlines was determined based on major changes of rock lithology and structure.

Fracture attributes recorded are, fracture types, attitude infill material, aperture and distance from the starting point of the scanlines. A total of 1128 fractures were surveyed along a total length of 238.0 m from seven (7) scanlines at Site 1, while, 629 fractures were surveyed along a total of 156.0 m from four (4) scanlines at Site 2. The length of scanlines varied from 20 to 48 m. Priest and Hudson [23] suggested that the length of scanlines must be at least fifty times the average spacing of discontinuities. The circular estimator method uses a combination of circular scanlines and windows.

According to Lyman [24] the method is a maximum likelihood estimator; it is therefore not subject to sampling bias [22]. The method can be used to estimate fracture attributes, by counting the number of intersections (n) between fractures and a circular scanline, as well as the number of fracture endpoints (m) located within the area defined by the scanline. According to Rohrbaugh et al. [25] a minimum of ten circular scanline surveys are required in a particular sampling area. Some useful definitions and equations of fracture density (ρ), fracture intensity (I), mean length (l) for linear scanline sampling and circular estimator methods are presented in Table 1.

3.3. Laboratory Work

The petrology of rocks of the TSU and the DGC has been described by Holm [26] and Nude et al [27]. The current petrological investigation was aimed at the texture and micro-structural characteristics of the major rock units. These characteristics can have significant influence on groundwater transmission and the mechanical properties of rocks [4,28].

Six rock samples were collected from the Site 1 and four from Site 2. However, thin sections were prepared from five (Table 5) of the most representative samples (three from Site 1 and two from Site 2) for subsequent mineralogical and petrographic investigation. The thin sections were examined using a petrological microscope under plane polarized light and crossed polarized light at the laboratory of the Department of Earth Science, University of Ghana, Accra, Ghana. Photomicrographs of the thin sections were taken.

Table 1. Summary of sampling methods, governing equations of fracture properties and the expected minimum measurements (Modified after [25])

Property		Definition	Scanline Sampling	Circular Estimator
Density (ρ)	Areal (P_{20})	Number of fractures per unit area [m^{-2}]	–	$\rho_{CE} = \frac{m}{2\pi r^2}$
Intensity (I)	Linear (P_{10})	Number of fractures per unit length [m^{-1}]	$I_{SLS} = \frac{N}{L}$	–
	Areal (P_{21})	Fracture length per unit area [mm^{-2}]	–	$I_{CE} = \frac{n}{4\pi}$
Spacing (S)	Linear	Spacing between fractures [m]	$S = \frac{1}{I_{SLS}}$	–
Mean length (lm)	Linear	Mean fracture length [m]	$1_{m;\,SLS} = \frac{\sum l}{N}$	$1_{m;CE} = \frac{\pi rn}{2m}$
Minimum number of measurements			225	860 [c]

N is the total number of sampled fractures, L is the scanline length, A is the sampling area, r is the radius of the circular scanline, l is the fracture length, n and m are the number of intersections with a circular scanline and the number of endpoints in a circular window enclosed by the circular scanline.. c Number of fractures contained in a sampling area.

Table 2. Scanline mapping

Linear					
Site	No of Scanline	Mean Azim (º)	Plunge (º)	Rock type	Length (m)
TSU	7	308	0	Quartzite/ phyllite/schist	34
DGC	4	133	0	Gneisses	39
Circular					
Site	No of Scanline	Radius (m)	Rock type		Area (m^2)
TSU	14	1.0	Quartzite/Phyllite/Schist		3.142
DGC	13	1.0	Gneiss		3.142

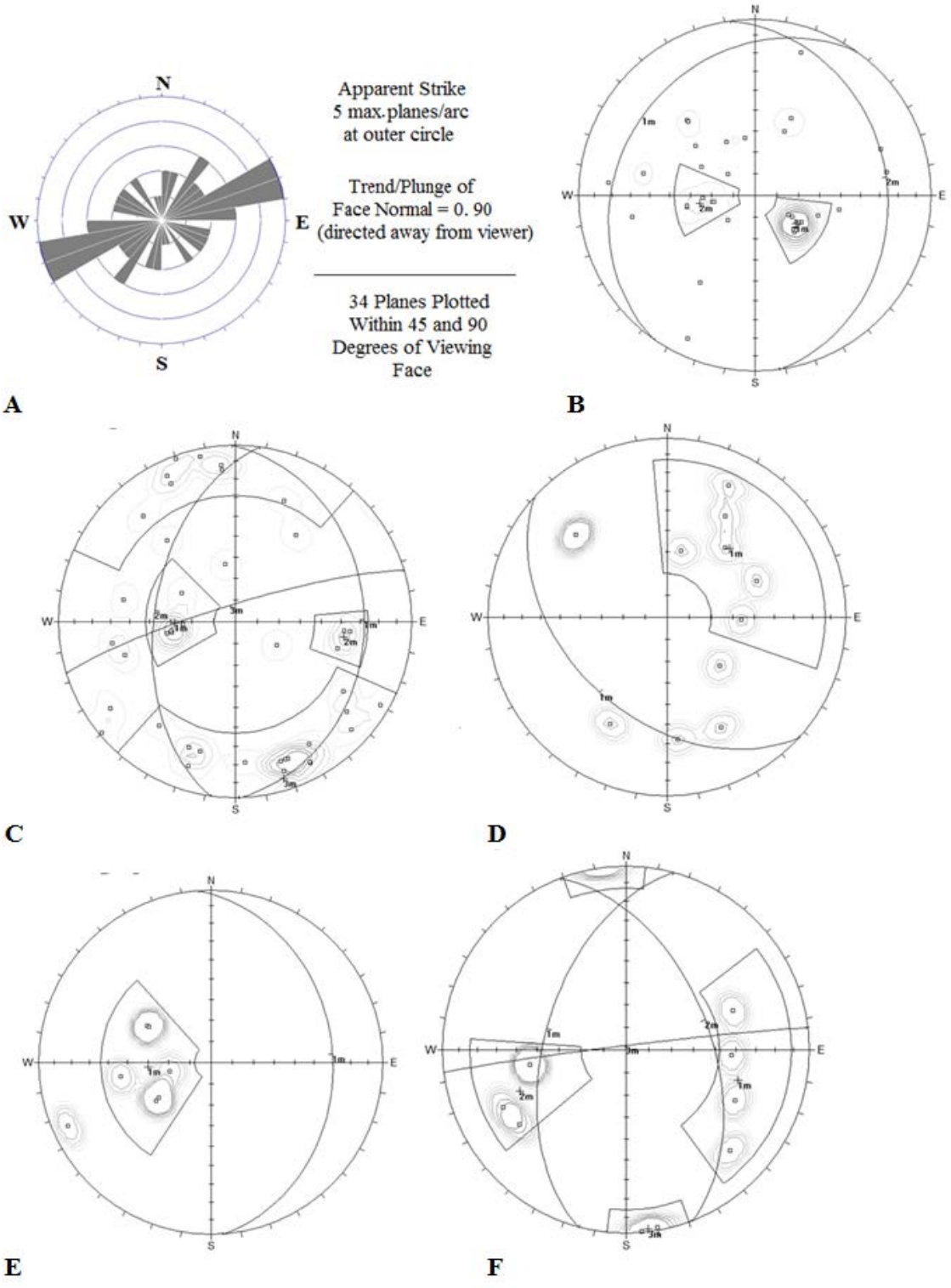

Figure 2. Equal Area Stereographic Projections of Structural Features Identified from Site 1, within the TSU. (A) Rose diagram joint and opened foliation planes, (B) Foliation sets within Quartzites, (C) Joints within the Quartzites (D) Fault sets within Quartzites at Site 1, (E) Foliation sets within the phyllite/Quartzite, (F) Joint sets within the phyllite/Quartzite

4. Results

Summary statistics of scanline surveys at Site 1 and Site 2 are presented in Table 2.

4.1. Fracture Data Analysis and Interpretation

Orientation and identification of fracture sets

Fractures are assumed to be planar [23] and so, the dip angle (the angle the plane makes with the horizontal surface), strike (the compass bearing a structural surface makes as it intersects the horizontal), and the dip direction (the compass bearing of the steepest line in the plane) uniquely define the orientation of the fracture. To identify fracture sets, dips and dip directions values recorded from linear scanlines were, imported into DIPS stereonet generating software described by Hoek and Diederichs [29].

Plots of .poles provided a visual depiction of pole concentrations. By contouring the pole plots, the most highly concentrated areas of poles, representing the dominant fracture sets were identified. The stereo-nets of the poles to planes of fracture orientations measured for outcrops at Site 1 and Site 2 are shown in Figure 2 and Figure 3 respectively.

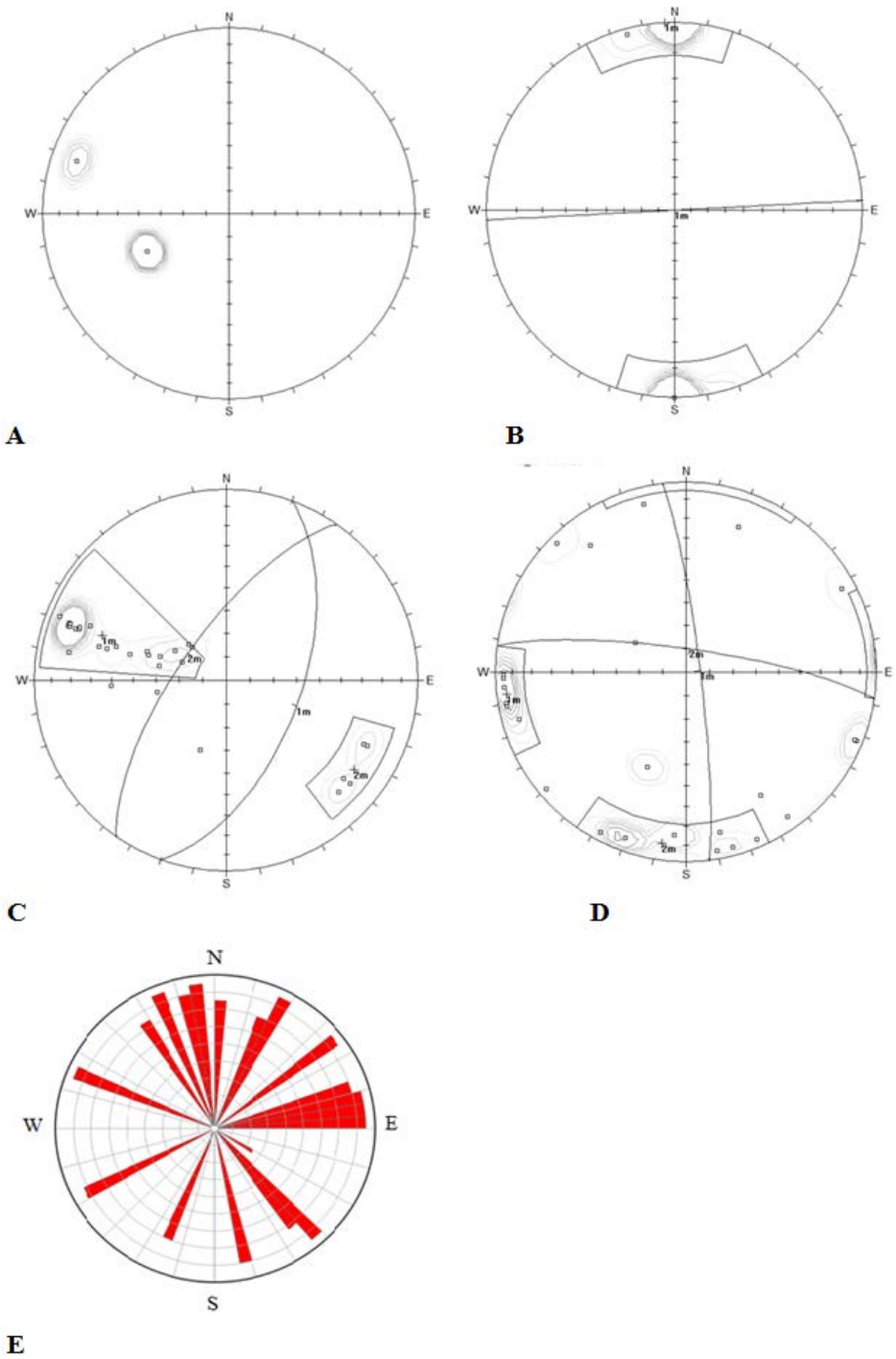

Figure 3. Equal Area Stereographic Projections of Structural Features Identified from Site 2, within the DGC. (A) Foliation sets within Acid gneisses site 2 (B) Joints sets within Acid gneisses site 2 [1 set], (C) , Foliation sets within basic gneisses at site 2 [2 sets], (D) Joints sets within basic gneisses site 2 [2 sets], (E) Rose diagram of fracture dip direction, indicating a very variable dip directions of joint system

Table 3. Mean orientation of fracture types from Sites

Rock type	Feature	Set	Orientation in (◦)
Quartzite (Site 1)	Foliation	1	23/305
		2	26/082
	Joints	1	20/089
		2	52/278
		3	82/343
	Faults	1	43/222
Phyllite/Quartzite intercalation (Site 1)	Foliation	1	30/086
	Joints	1	53/285
		2	52/069
		3	88/353
Acid gneiss (Site 2)	Foliation	-	-
	Joints	1	90/177
Basic gneiss (Site 2)	Foliation	1?	58/110
		2	70/305
	Joints	1	84/083
		2	80/008

Table 3 present summaries of the mean orientations of the various fracture types from the Site 1 and Site 2, respectively.

4.2. Fracture Frequency, Spacing and Spacing Distribution

The frequency of a fracture set (λ) can be defined as the number of fractures per unit length (for 1D analysis), the number of discontinuities per unit area (for 2D analysis) or per unit volume (for 3D analysis). Fracture spacing (S) is the inverse of frequency (i.e. λ^{-1}). Total fracture spacing (S) is defined as the distance between a pair of immediate adjacent fractures intersecting with the measuring scanline [21,23].

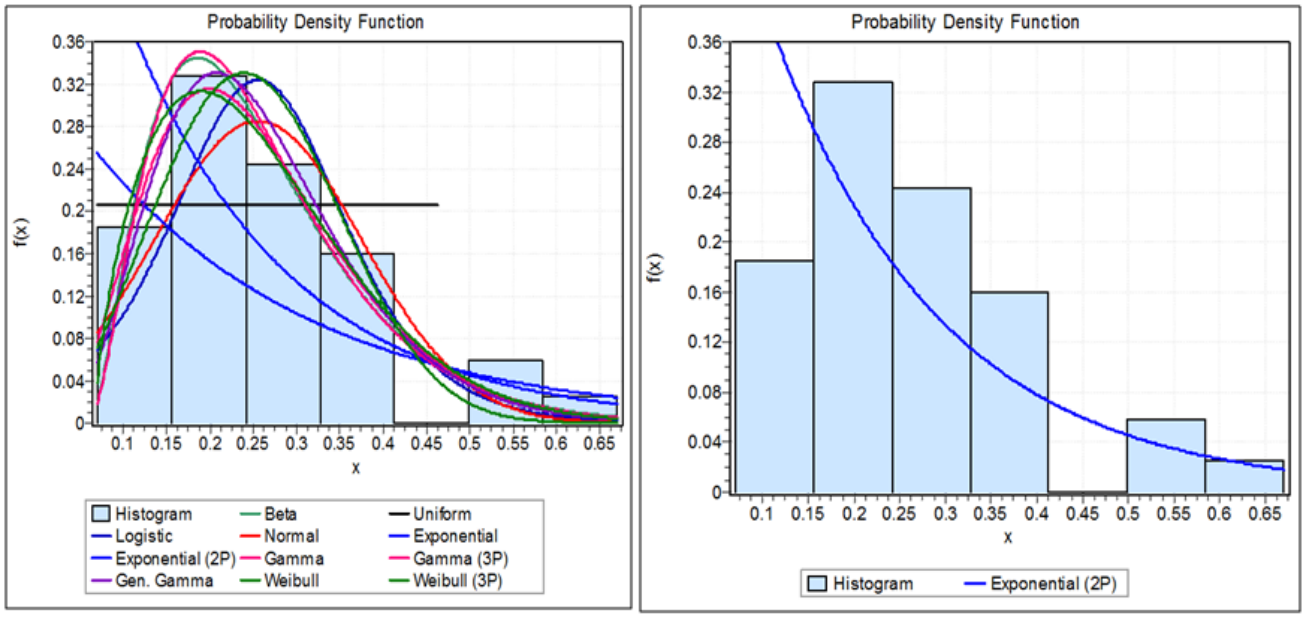

Figure 4. Histogram and total fracture distribution for Ablekuma linear scanline mapping: (a) Possible distribution models, (b) Best fit model

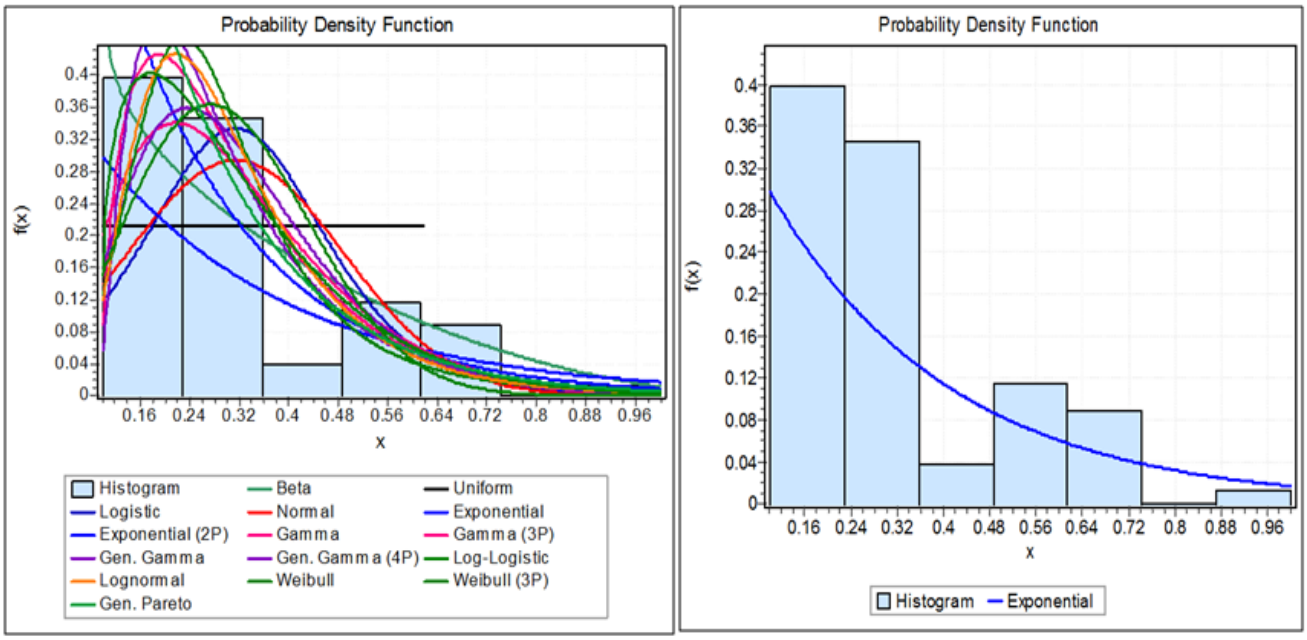

Figure 5. Histogram and total fracture distribution for Danfa linear scanline mapping: (a) Possible distribution models, (b) Best fit model

An analysis of fracture spacing data was carried out to determine the fracture total spacing distribution for the two study sites. The best fit models for the two sites are shown in Figure 4 and Figure 5, and the results of statistical analysis are summarised in Table 4. Distribution forms for both Site 1 and 2 indicated negative exponential distributions, which is in agreement with Priest and Hudson [23], Wallis and King [30] for most fracture spacing analysis. For best fit distribution analysis, the Easy Fit software [31] was used. Site 1 showed a negative 2-parameter exponential function, while, that of Site 2 was simply a negative exponential probability density function (pdf). The 2-parameter exponential probability density function (pdf) is given by:

$$f(x) = \lambda e^{-\lambda(x-\gamma)}, \quad \text{for } f(x) \geq 0, \lambda > 0, x \geq 0 \text{ or } \gamma. \tag{1}$$

where, λ is the frequency or fracture per unit length; The value of λ was determined as 5.3895 fracture/m, and γ as 0.07. For Site 2, the negative exponential distribution is expressed as:

$$f(x) = \lambda e^{-\lambda x} \tag{2}$$

where, f(x) is the frequency of fracture spacing x, and λ is the average number of fractures per metre. This is a one parameter (λ) distribution with the mean and standard deviation (SD), both equal to $\frac{1}{\lambda}$. λ was determined as 3.1811.

4.3. Intensity and Density

There are different parameters used for describing the quantity of fractures in rocks. Fracture intensity (I) is one of the most commonly determined parameter from one-dimensional observation domains (i.e. scanlines). It is obtained by dividing the number of fractures (N) by the total length (L) of the scanline:

$$Fl = \frac{N}{L}. \tag{3}$$

This expression is the same as linear fracture density (d_1 or P_{10}), which is defined as, the average number of fractures per unit length. The linear fracture intensity (P_{10}) for Site 1 was computed as 4.739 fractures/m 1128 fractures along 238.0 m scanline length, and 4.030 fractures/m from 629 fractures along a total of scanline of 156.0 m for Site 2.

4.4. Fractures Mean Trace Length

The size of fractures is an important but difficult parameter to determine [32], due to the fact that, fracture traces often one or both ends censored in the outcrop. In this study, the approach (circular scanline) proposed by Rohrbaugh et al [25] was used to determine the mean trace lengths for Site 1 and.2. The approach was used, not only to eliminate orientation bias observed in rectangular window sampling, but also to reduce time spent on data collection. The overall mean trace length was computed from 14 circular scanlines at Site 1 as 2.589 m, and 2.881 m for Site 2 (Table 4).

Table 4. Summary statistics of circular scanlines and mean trace lengths from Sites

Circular Scanline ID	Parameter				
Sites	n	m	Density (ρ)	Mean length (l_m) m	Intensity (I) n/4r (m)
CSLAB001_S1	51	25	3.98	3.203	12.75
CSLAB002_S1	39	19	3.03	3.223	9.75
CSLAB003_S1	34	25	3.98	2.135	8.50
CSLAB004	35	17	2.71	3.232	8.75
CSLAB005	38	25	3.98	2.386	9.50
CSLAB006	55	30	4.78	2.878	13.75
CSLAB007	60	47	7.48	2.004	15.00
CSLAB008	86	89	14.17	1.517	21.50
CSLAB009	91	68	10.82	2.101	22.75
CSLAB010	56	41	6.52	2.144	14.00
CSLAB011	31	11	1.75	4.425	7.75
CSLAB012	15	22	3.50	1.070	3.75
CSLAB013	72	48	7.64	2.355	18.00
CSLAB014	75	39	6.21	2.569	18.75
		Overall	**5.57**	**2.589**	**13.18**
CSLDA001_S2	24	22	3.50	1.714	6.00
CSLDA002_S2	38	18	2.87	3.314	9.50
CSLDA003_S2	42	25	3.98	2.536	10.50
CSLDA004	40	11	1.75	5.709	10.00
CSLDA005	49	26	4.14	2.959	12.25
CSLDA006	45	30	4.78	2.355	11.25
CSLDA007	43	26	4.14	2.577	10.75
CSLDA008	48	32	5.10	2.355	12.00
CSLDA009	49	38	6.05	2.024	12.25
CSLDA010	35	16	2.55	3.434	8.75
CSLDA011	22	19	3.03	1.818	5.50
CSLDA012	29	13	2.07	3.502	7.25
CSLDA013	30	15	2.39	3.140	7.50
		Overall	**3.57**	**2.881**	**9.50**

'*r*' is the radius of the circular scanline, *l* is fracture trace length, *n* and *m* are the number of intersections with a circular scanline and the number of endpoints in a circular window enclosed by the circular scanline.

Table 5. List of rock samples used for petrographic investigation

Study Site	Sample ID	UTM East/UTM North	Rock type
1	TSU1001	0623657/30 N 0800849	Quartzite
1	TSU1002	0623943/30 N 0800940	Quartzite
1	TSU1003	0623610/30 N 0800891	Schist
2	TSU1004	0640301/30 N 0816111	Basic gneiss
2	TSU1005	0640723/30 N 0814453	Acidic gneiss

Laboratory microstructural investigation of thin sections of rock units of the study area are complementary to the study of the surface structure. The following are brief descriptions of the microscopic investigation of the dominant rock units.

4.4.1. Quartzites and Schist of the TSU

Quartzite: At the hand specimen scale, the rocks appear as light grey to whitish grey medium to coarse grained massive mass. Microscopically, the rock is medium to coarse grained, foliated and exhibits proto-mylonitic textures. It is composed predominantly of quartz and alkali feldspars (orthoclase), sericite, and apatite. Quartz

grains are elongated, cryptocrystalline and undulose. They usually exhibit flat to sub-sutured boundaries and show preferential orientation. Alkali feldspars have been completely or partially altered into sericite and are mostly found between the boundaries of the quartz crystals. Apatite is sub-hedral to anhedral and may have inclusions of fine grained rounded quartz which occur as quartz impregnations. In term of micro-structural interpretation, it can be said that, this is highly sheared metamorphic rock of quartzo-feldspathic protolith. It is foliated, highly strained and deformed with presence of micro-faults which have displaced some of the grains. Micro-faults are mostly discordant to foliation planes. In some cases the elongated quartz grains are also fractured.

Schist: These rocks were probably second to quartzites at Site 1 in terms of abundance. The rocks appear as dark-grey to greenish, fine to medium grained and strongly foliated at hand specimen scale. Under the microscope, the rock specimen has a mineralogical composition of dominant sericite (Ser), chlorite (Chl), some muscovite (Ms), quartz (Qtz) and some epidote. The mineral grains are very fine. The visible grains are elongated and lineated due to shearing.

The specimen has two kind of zones, which consists of chloritic and serictic zones. The sericitic zones contain some large quartz grains sieves that are less sheared as compared to the chloritic zones, which are severely sheared. A fracture was observed in the specimen, which trends in the direction of the mineral foliation. The difference in the severity of the shearing could be as a result of relative abundance of quartz in some zones more than others.

4.4.2. Basic gneiss of the Dahomeyan

The amphibolite-grade Dahomeyan gneisses consist of strongly foliated, interlayered leucocratic and melanocratic components. In thin section, the rock is medium grained and weakly foliated. It is composed of quartz, alkali feldspars (perthite and orthoclase), plagioclase, chlorite, sericite, apatite and opaque minerals. Quartz may be monocrystalline and polycrystalline and exhibits undulose extinction. In most cases the quartz crystal are elongated with sutured grain boundaries. Figure 6 are examples of microscopic observations.

4.4.3. Computed Fracture Set Properties for the Study Sites.

The commonly used geometric properties for the characterisation of fracture networks include fracture, orientation, spacing and frequency, intensity, density, mean length and fracture length distribution [21,22,33,34].

4.5. Orientation and Fracture Sets

Joints and foliations are the most common fracture types at both Site 1 and 2. There is also a number of quartz veins at Site 2. From stereographic plots (Figure 2 and Figure 3), it was shown that, at least two sets of fractures occur for both joints and foliation planes in all the rock types. Joints within the quartzites of Site 1 indicates three fracture populations: two major populations (58% and 35%) and a minor one (7%). The most dominant joint set is steeply dipping (>75º). They are probably columnar joints. Foliation planes at Site 1 generally dip gently (< 30°). The joints do not appear to change their direction with the dip and strike of foliation planes and bedding in the quartzites, an indication they could be of younger generation. They seem to be closely related (at right-angles) to the northeast-trending regional folds as reported by De Sitter [35].

From rose diagram of combine joints and opened foliations (Figure 2A), fractures at Site 1 generally trend east-northeast (060-080), north-northeast (010-020°) (12%), and east-southeast (100-110°). Dips of fractures within the acidic and basic gneisses at Site 2 were variable as shown in rose diagram (Figure 3). Fracture sets were characterised mainly according to their trends. The dominant strike of the foliation is north-northeast (015-039°) dipping gently (35-40°) to the southeast.

Two major joints sets were identified. The dominant set striking 290°, and dipping steeply (85°) southeast, while the subordinate set, dipping moderately (58°) southest and striking 260°. Most fracture dips are sub-perpendicular to foliation planes. Fracture sets were characterised mainly according to their trends. Most joints within the gneisses are filled and sealed with quartz and other minerals (e.g. hematite, limonite, etc.).

4.6. Fracture Frequency, Spacing and Spacing Distribution

The linear fracture frequency, mean fracture spacing, fracture density and intensity measured linearly along the scanline is presented in Table 6. The mean linear density indicates a close level of fracturing (>4 fractures/m) for the two study sites, albeit maximum spacing was 1.0m at Site 2.

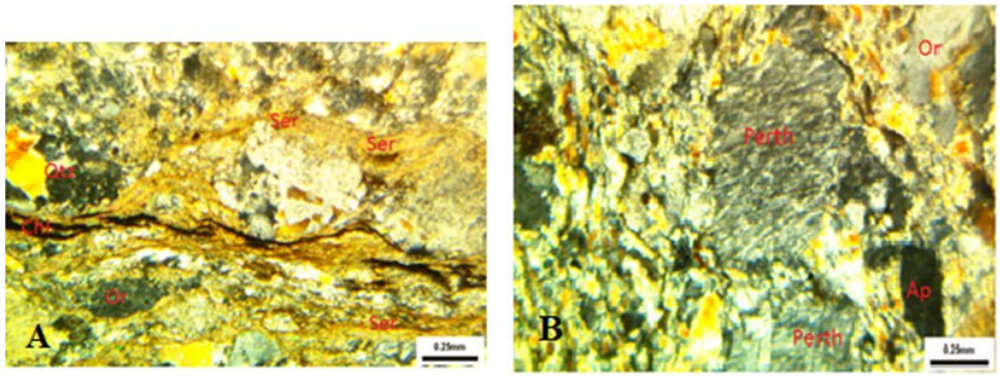

Figure 6. Photomicrograph of Sample TSU 1004 (A) Strongly Deformed Rock Showing Preferred Oriented Mineral Grains, and Alteration Features. (B) Micro-texture Showing Coarse and Micro-perthites and Deformed Fine Grained Quartz (Crossed Polars)

Table 6. Comparison of fracture characteristics from Site 1 and Site 2

Fracture parameter	Study site	
	Site 1 (TSU)	Site 2 (Dahomeyan)
Total scanline length (m)	238.0	156.0
Total number of surveyed fractures (N) from linear scanl.	1128	629
Mean spacing (m)	0.256	0.314
Min. (m)	0.07	0.10
Max. (m)	0.67	1.00
SD for spacing	0.12	0.18
COV, spacing	0.47	0.58
Linear frequency (λ) (frac/m)	5.390	3.181
Mean trace length (lm)	2.589	2.881
Areal density (ρ) (Frac/m^2)	5.57	3.57
Intensity (I)	13.18	9.50

Comparing the means of fracture spacing for both Site 1 (TSU) and Site 2 (Dahomeyan formation) with ISRM (1978) (Table 7), fractures in both sites can be said to have close to moderate fracture spacing. This has important implication on fluid flow and geotechnical properties of the rock masses.

Table 7. Classification of fracture spacing [36]

Description	Spacing (mm)
Extremely close spacing	< 20
Very close spacing	20 - 60
Close spacing	60 - 200
Moderate spacing	200 -600
Wide spacing	600 - 600
Very wide spacing	2000 - 6000
Extremely wide spacing	> 6000

The form of the raw fracture spacing values at Site 1, were such that, they could best be fitted with negative 2-parameter exponential density function model (Figure 4). The 2-parameter exponential probability density function (pdf) is given by:

$$f(x) = \lambda e^{-\lambda(x-\gamma)}, \quad \text{for } f(x) \geq 0, \lambda > 0, x \geq 0 \text{ or } \gamma \tag{1}$$

where, λ is the frequency or fracture per unit length. The value of λ was determined as 5.3895 fracture/m and γ as 0.07. Equation for the fracture spacing distribution at Site 1 is thus given by:

$$f(x) = 5.390e^{5.390(x-0.07)}, \; x \geq 0.$$

For Site 2, the best fit form of distribution model for the raw fracture spacing values was, negative exponential probability distribution function, expressed mathematically as:

$$f(x) = \lambda e^{-\lambda x} \tag{3}$$

where, f(x) is the frequency of fracture spacing x, and λ is the average number of fractures per metre. This is a one parameter (λ) distribution with the mean and standard deviation (SD), both equal to $\frac{1}{\lambda}$. λ was determined as 3.1811. The overall mean fracture spacing for Site 1 was 0.256 m, and that for Site 2 was 0.314 m.

4.7. Areal Intensity, Density and Trace Length

The areal fracture intensity (P_{10}), computed from circular scanline survey was 13.18 and 9.50 for Site 1 and 2 respectively. Overall mean trace length for Site 1 and 2, determined from circular scanline survey data was 2.589 m, and 2.881 m (Table 6) respectively. Comparing the values of fracture intensity, mean trace lengths, and fracture spacing from the two sites, it is clear fracturing is more intense at Site 1 within the TSU than Site 2 in the Dahomeyan Formation.

4.8. Micro-structural Analysis

Micro-structural investigation of the main rock type in at Site 1 (TSU), quartzite was found to be highlyfoliated, highly strained and deformed with presence of micro-faults which have displaced some of the grains. Micro-faults are mostly discordant to foliation planes. In some cases the elongated quartz grains are also fractured. This can have effect on fluid flow and contaminant transport in this rock unit [4,15]. The Dahomeyan gneisses are plutonic rocks, metamorphosed and foliated. The rocks are strongly deformed with deformation been both ductile and brittle. This rock has probably been caught-up in a sheared which has resulted in the elongated and preferred orientation of its constituent grains.

5. Conclusions and Recommendation

The approach of field geological mapping, linear and circular mapping, and laboratory investigation of micro-structures in rock units from the study area were used to characterise fractures at Site 1 (TSU) and Site 2 (DGC). One of the important elements in the selection of dumpsites and landfill sites is the geology of the site, and in evaluating the suitability of an area, the potential of groundwater contamination is paramount. Comparing results of fracture characteristics and petrographic studies from the dominant rock types at Site 1 and 2, it can be concluded that rocks at Site 1 are more intensely fractured and less intact than those at Site 2. Fractures at Site 1 are predominantly opened compared to those of Site which are filled or cemented with quartz veining. The Dahomeyan Gneissic Complex would thus be more suitable for the selection of waste disposal sites than the

Togo structural units. Furthermore, considering the fact that, groundwater is a major source of water supply for domestic, industrial, and agriculture of many communities within the study area, proper geological and hydrological data collection and data management practices are recommended, if the management and protection of groundwater resources in the Accra-Tema area are to be achieved.

References

[1] Rao, K. S. (1997). Site selection for a landfill. Narosa Publishing House, New Delh.

[2] Dorhofer, G. and Siebert, H. (1998). The search for landfill sites requirements and implementation in Lower Saxony, Germany. Environ Geol. 35: 55-65.

[3] Dorn, M, Tantiwanit, W. (2001). New methods for searching for waste disposal sites in the Chiang Mai–Lamphun basin, Northern Thailand. Environ Geol. 40: 507-517.

[4] Brace, W. F. (1980), Permeability of crystalline and argillaceous rocks, Int. J. Rock. Mech. Min. Sci. Geomech. Abstr. 17, pp. 241-251.

[5] Simsek, C., Kincal, C., and Gunduz, O. (2006). A solid waste disposal site selection procedure based on groundwater vulnerability mapping. Environ Geol 49: 620-633.

[6] UNEP-IETC and HIID (1996), "International Source Book on Environmentally Sound Technologies for Municipal Solid Waste Management", United Nations Environment Programme (UNEP), Osaka/Shiga.

[7] Lorah, M. M., Cozzarelli, M. I. and Boehlke, J., (2009). Biogeochemistry at a wetland sediment-alluvial aquifer interface in a landfill leachate plume, Journal of Contaminant Hydrology, 105(3-4), 99-117.

[8] Machiwal, D., and Jha, M. K. (2010). Tools and techniques for water quality interpretation. In: Krantzberg, G., Tanik, A., Antunes do Carmo, J.S., Indarto, A., Ekdal, A. (Eds.), Advances in Water Quality Control. Scientific Research Publishing, Inc., California, USA, pp. 211-252.

[9] Stinnette, D. S. (1996), "10 Steps to Successful Facility Siting," Waste age, Internet Available: http://wasteage.com.

[10] Sadek, S. Mutasem, E. F. and Fadel, F. (2006), "Compliance Factors within A GIS-Based Framework for Landfill Siting," International Journal of Environmental Studies, Vol. 63, No. 1, 2006, pp. 71-86.

[11] Paraskevopoulos, A., Geogiadis, Th., and Geogiadou, M. (1992), Environmental Impact Assessment Study for the development of landfill site at North East Attica.

[12] Petts, J., and Eduljee, G. (1994), Environmental impact assessment for waste treatment and disposal facilities. Chichester: Wiley.

[13] Daly, D. (1983). Co-disposal sites selection, investigation, and monitoring. Proceedings of seminar "Local authority experience in implementation of water and waste legislation". Dun Laoghaire. 16pp.

[14] Anon (1997) Consultancy for the study of the ATMA development and Investment programme and of the Rehabilitation/Replacement of Kpong-Tema-Accra water pipeline, pp. 4-21.

[15] Muff, R., and Efa, E., (2006). Explanatory Notes for the Geological Map for Urban Planning 1:50 000 of Greater Accra Metropolitan Area. 38p.

[16] Dickson, K. B., and Benneh, G. (1988). A New Geography of Ghana, Longman Group (FE) Ltd, 170 p.

[17] Kesse, G. O. (1985). The mineral and rock resources of Ghana. A. A. Balkema Publishers, The Netherlands, 610p.

[18] Kuma, J. S. and Ashley, D. (2008). Runoff estimates into the Weija Reservoir and its implications for water supply to Accra, Ghana. Journal of Urban and Environmental Engineering, v.2, n.2, pp. 33-40.

[19] Dapaah-Siakwan, S., and Gyau-Boakye, P. (2000). 'Hydrologic framework and Borehole yields in Ghana'. Hydrology Journal, Vol. 8 pp 405-416

[20] Darko, P. K. (2001), *Quantitative Aspects of Hard Rock Aquifers: Regional Evaluation of Groundwater Resources in Ghana*. Ph.D Thesis, Charles University, Prague, Czech Republic.

[21] Priest, S. D. (1993), Discontinuity analysis for rock engineering: London, United Kingdom, Chapman & Hall, 473.

[22] Mauldon, M., Dunne, W.M., Rohrbaugh Jr., M. B., (2001). Circular scanlines and circular windows: new tools for characterizing the geometry of fracture traces. Journal of Structural Geology 23, 247-258.

[23] Hudson, J. A. and Harrison, J. P. (1997), Engineering rock Mechanics: An introduction to the principles. Published by Elsevier Science Ltd. 444pp.

[24] Lyman, G. J. (2003). Rock fracture mean trace length estimation and confidence interval calculation using maximum likelihood methods. International Journal of Rock Mechanics and Mining Sciences 40, 825-832.

[25] Rohrbaugh Jr, M. B., Dunne, W. M., Mauldon, M., (2002), Estimating fracture trace intensity, density and mean length using circular scanlines and windows. AAPG Bulletin 86, 2089-2104.

[26] Holm, F .R. (1974). Petrology of alkalic gneiss in the Dahomeyan of Ghana. *Geological Society of America Bulletin*, 85, pp 1441-1448.

[27] Nude, P. M., Shervais, J., Attoh, K., Vetter, S. K., and Barton, C. (2009), Petrology and geochemistry of nepheline syenite and related carbonate-rich rocks in the Pan- African Dahomeyide orogen, southeastern Ghana, West Africa. *Journal of African Earth Sciences*, 55, pp 147-157.

[28] Brown, S.R. (1989). Transport of fluid and electric current through a single fracture, J. Geophys. Res., 94, 9429-9438.

[29] Hoek, E, Diederichs, M. S. (1989). Dips User Manuel. University of Toronto.

[30] Wallis, P. F. and King, M. S. (1980). Discontinuity spacing in a crystalline rock. International Journal of Rock Mechanics and Mining Sciences and Geomechanics Abstracts; 17(1):63–66.

[31] Schittkowski, K. (EASY-FIT 2002): A software system for data fitting in dynamic systems. Struct. Multidisc Optim. 23, pp. 152-169. Springer-Vertag

[32] Cacciari, P. P. and Futai, M. M. (2015). Mapping and characterization of rock discontinuities in a tunnel using 3D terrestrial laser scanning. Bulletin of Engineering Geology and the Environment.

[33] Pahl, P. J. (1981), Estimating the mean length of discontinuity traces: International Journal of Rock Mechanics and Mining Sciences and Geomechanics Abstracts, Vol. 18, pp. 221-228.

[34] Neuman, S. P. (2005), Trends, prospects and challenges in quantifying flow and transport through fractured rocks: Hydrogeology Journal, Vol. 13, pp. 124-147.

[35] Sitter, L. U. de, (1956). Structural Geology: New York, McGraw-Hill Book Co., 552 p.

[36] International Society for Rock Mechanics (ISRM) (1978), Suggested methods for the quantitative description of discontinuities in rock masses. Int. Jour. Rock Mech. Min. Sci. Geomech. Abstr. 15:pp. 319-368.